Preparation of two-photon fluorescent probe and biological imaging application in cells

Shuheng Chi (迟书恒)[1], Liang Li (李 亮)[1], and Yiqun Wu (吴谊群)[1,2,*]

[1]*Key Laboratory of Material Science and Technology for High Power Lasers, Shanghai Institute of Optics and Fine Mechanics, Chinese Academy of Sciences, Shanghai 201800, China*

[2]*Key Lab of Functional Inorganic Material Chemistry (Heilongjiang University), Ministry of Education, Harbin 150080, China*

**Corresponding author: yqwu@siom.ac.cn*

Received December 19, 2015; accepted April 15, 2016; posted online May 30, 2016

We report on a novel dibenzothiophene-based two-photon fluorescent probe for selective nuclear bioimaging, which contains bilaterally symmetrical pyridine rings connected by a central conjugated-bridge dibenzothiophene. This probe possesses a large two-photon absorption cross-section of 471 GM, yields a 25-fold enhancement of the fluorescence titration, and a stronger photostability for nuclei labeling than existing probes. The real-time observation period is a minimum of 1800 s under a femtosecond laser excitation, which is significantly longer than that of 4′,6-diamidino-2-phenylindole. The above results confirm that this novel molecule is a suitable two-photon fluorescent probe for application to nuclear bioimaging in cells.

OCIS codes: 160.0160, 160.4670, 160.2540, 190.4400, 180.2520, 170.3880.
doi: 10.3788/COL201614.061603.

With the development of microscopic imaging technology, optical confocal fluorescence microscopy has become a powerful tool for the observation and research of living cells and tissues[1]. Compared to traditional one-photon optical microscopy, two-photon fluorescence microscopy is an important technique that supports the ongoing development of life science through the provision of unique advantages. Specifically, two-photon fluorescence microscopy provides a near infrared (near-IR) excitation light source, a low damage threshold, deep penetration, and a highly three-dimensional spatial selectivity[2–4]. However, the potential applications of two-photon bioimaging in cells, especially in nuclei, are significantly hindered by a lack of excellent fluorescent probes with large two-photon absorption (TPA) cross-sections, high fluorescence quantum yields, accurate selective localization ability, and good photostability in real-time monitoring. To date, a number of two-photon fluorescent probes with various morphologies and functions has been reported, such as carbon nanodots, cyclometalated complexes, ratiometric pH sensors, ion probes, and cyanine fluorophores[5–9]. However, despite the fact that these fluorescent dyes exhibit favorable photophysical properties and specific selectivities and localizations, insufficient attention has been paid to organic small molecule labeling in the scientific field of two-photon excited fluorescence (TPEF) bioimaging. It is particularly noteworthy that these dyes exhibit nuclear labeling ability and photostability that is competitive with commercial fluorescent dyes. Considering the important roles of gene regulation and nucleus protection in biological tissue and organs, the development of novel, organic, two-photon fluorescent probes for nuclear DNA imaging with excellent TPA performance is an urgent and important priority[10,11].

Herein, we report a novel dibenzothiophene-based two-photon fluorescent probe (TPI) for selective cellular nuclei imaging (Scheme 1). The rigid structure of the overall delocalized conjugated system enhances the TPA properties of the molecule, and the unilateral quaternization of the pyridine cation further enables the two-photon excitation wave band to shift within the near-IR biological optical window, which is beneficial for the realization of clear TPEF bioimaging. In addition, the one- and two-photon photophysical properties, the luminance "turn-on" effect, two-photon bioimaging, and the microscopic DNA binding mechanism are explored and discussed in detail. To comprehensively reflect the performance advantages of the synthetic probe presented herein, a commercial fluorescent dye known as 4′,6-diamidino-2-phenylindole (DAPI), which has a superior nuclear labeling ability, is employed as a reference. The experimental results demonstrate that this novel small-molecular compound is an outstanding two-photon fluorescent probe with a large TPA

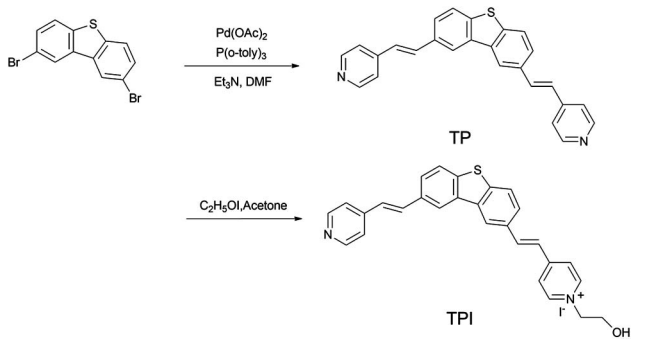

Scheme 1. Synthesis of dibenzothiophene-based fluorescent probe.

cross-section, good membrane permeability, and high photostability for highly selective nuclear imaging.

The 2,8-dibromodibenzothiophene was purchased from Alfachem. Co. (Zhengzhou, China). The 4-vinylpyridine was purchased from Alfa Aesar (USA). Other reaction raw materials and reagents were obtained from Sinopharm Chemical Reagent Co., Ltd (Shanghai, China). DAPI and MitoTracker Red CMXRos (MTR, a commercial red mitochondrial staining reagent) were purchased from Invitrogen (USA). A tris(hydroxymethyl)aminomethane (Tris) -HCI buffer solution was formulated as a mixture of 10 mmol Tris and 100 mmol NaCl at a pH of 7.4. The TPI and DNA were added to the buffer solutions at concentrations of 10^{-5} and 0–1.3×10^{-3} mol/L, respectively, and these solutions were preserved at 4°C before use.

The ultraviolet (UV) absorption spectra were obtained using a HITACHI UH5300 spectrophotometer, and the one-photon excited fluorescence (OPEF) spectra were recorded using an FP-6500 fluorescence spectrometer. The fluorescence quantum yield (Φ) values were obtained using Rhodamine B in ethanol at 25°C as a reference. The TPEF spectra were recorded using a 7ISW301 fluorescence spectrometer equipped with a 7IDA1 data acquisition unit and a 7IP1100 high voltage regulated power supply. The concentration of the unknown and reference samples in the measurement of OPEF and TPEF spectra was unified to 10^{-5} and 10^{-4} mol/L, respectively. A mode-locked Ti:sapphire pulse laser (repetition rate: 80 MHz, pulse duration: 80 fs) was used as a pump radiation source. The TPA cross-section (σ) values were calculated based on the two-photon induced fluorescence method[12], which states that

$$\sigma_s = \sigma_r \frac{F_s}{F_r}\frac{\varphi_r}{\varphi_s}\frac{c_r}{c_s}\frac{n_r}{n_s}, \tag{1}$$

where the subscripts s and r represent the unknown and reference materials, respectively; F is the two-photon integral fluorescence intensity; c and n refer to the concentration and refractive index of the examined solution, respectively.

3T3 mouse myoblasts were grown in a Dulbecco's modified eagle medium (DMEM) under 5% CO_2 for 12 h at 37°C. The medium was then incubated by adding a permeabilization buffer and blocking solution, sequentially, and washed with a phosphate-buffered saline (PBS) solution repeatedly (three times). Finally, the cells for bioimaging were stained with TPI and DAPI in a process conducted at 37°C for 15 min.

The one- and two-photon fluorescence imaging was conducted on an LSM 710 (Carl Zeiss) confocal scanning microscope. The excitation wavelength of the OPEF imaging for the TPI was 405 nm, whereas the excitation wavelengths of the TPEF imaging for TPI and DAPI were 800 and 740 nm, respectively. Three optical windows (channel I: 410–490 nm, channel II: 525–575 nm, and channel III: 585–660 nm) were set in order to collect the fluorescence emitted from the DAPI, TPI, and MTR, respectively.

The following preparation method was employed in order to obtain the novel TPI compound. First, 2,8-dibromodibenzothiophene (5.12 g, 0.015 mol), 4-vinylpyridine (6.30 g, 0.060 mol), tri(o-tolyl)phosphine (0.91 g, 0.003 mol), and palladium acetate (0.13 g, 0.6 mmol) were uniformly added to a pressure-tight reaction vessel, which was filled with high purity nitrogen. Then, the temperature was gradually increased to 120°C under continuous magnetic stirring. After 15 h of reaction, the container was cooled to room temperature. A intermediate product 2,8-bis((E)-2-(pyridin-4-yl)vinyl) dibenzothiophene (TP) was obtained via extraction by dichloromethane and silica gel column chromatography by ethyl acetate-petroleum (3:1). Secondly, TP (3.90 g, 0.010 mol), iodoethanol (2.58 g, 0.015 mol), and acetone (35 mL) were added to a small round bottom flask, and a quaternization reaction was then conducted at 80°C under uniform stirring for 12 h. Finally, the major product, i.e., TPI, was obtained via vacuum filtration, further washing, and blast drying. Yield: 3.46 g (69%), 1 H NMR (400 MHz, DMSO-d6, ppm): 9.03 (d, $J = 6.1$ Hz, 2 H), 8.95 (s, 2 H), 8.61 (m, 2 H), 8.29 (d, $J = 2.9$ Hz, 2 H), 8.27 (s, 2 H), 8.18 (d, $J = 5.4$ Hz, 2 H), 8.14 (m, 2 H), 8.01 (m, 2 H), 7.90 (d, $J = 4.4$ Hz, 2 H), 4.86 (m, 2 H), and 3.53 (s, 3 H). 13 C NMR (125 MHz, DMSO-d6, ppm): 59.9, 62.1, 121.1, 123.2, 123.6, 127.9, 132.3, 135.3, 140.2, 140.9, 144.5, and 152.9. FT-IR (KBr) γ (cm^{-1}): 3285 (C-H, pyridine), 1615 (C = N, pyridine), and 971 (= C-H, ethylene). MALDI-TOF-MS: m/z ($C_{28}H_{23}N_2OS$), found: 435.149 $[M\text{-}I]^+$.

To investigate the OPEF photophysical properties of TPI, its UV absorption and OPEF spectra were measured, as shown in Fig. 1. It is apparent that the absorption wavelength was red-shifted to ~400 nm following the quaternization reaction, while the fluorescence wavelength was located in the green spectral region, corresponding to a Stokes shift of ~150 nm. This shift was more than

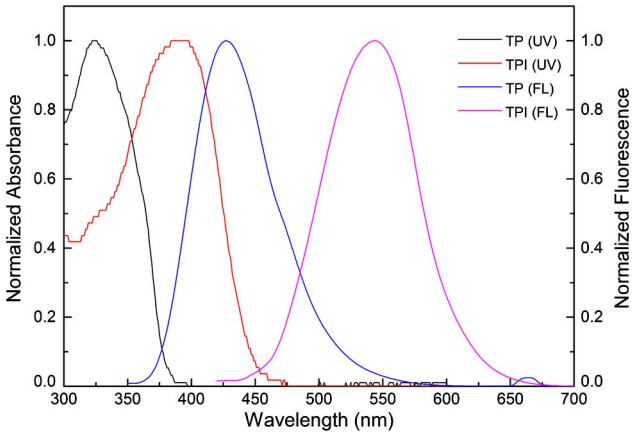

Fig. 1. Normalized UV absorption and one-photon fluorescence (FL) spectra of TP and TPI in DMF, [TPI] = 10^{-5} mol/L.

that of the DAPI (only ~50 nm) and was due to the large π-conjugated delocalized plane of TPI. The Φ was 0.52, corresponding to a good OPEF performance. This can be attributed to the high intramolecular charge transfer efficiency through the entire conjugated system[13,14]. The location of the UV absorption wavelength (~400 nm) indicates that the TPA phenomenon may be induced by femtosecond laser excitation at an 800 nm wavelength, which is considered to be the comfortable near-IR optical window for two-photon bioimaging.

To explore the TPEF photophysical properties, the two-photon fluorescence spectra of TPI and DAPI in N, N-dimethylformamide (DMF) solutions were measured (Fig. 2). The TPEF intensity of the TPI was significantly greater than that of DAPI, with a difference of almost an order of magnitude. Through calculation, the σ of the TPI was found to achieve ~471 GM, which is almost 1000 times higher than that of DAPI (only ~0.46 GM). The TPA action cross-section ($\sigma_a = \sigma\Phi$) reached ~245 GM. Compared with some other recently reported fluorescent probes, e.g., pyridine cation derivative[15], $\sigma_a = 152$ GM; polypyridyl complexes[16], $\sigma_a = 13 - 20$ GM; curcumin derivative[17], $\sigma_a = 104$ GM, it demostrated that the TPI had a higher TPA action cross-section. This can be attributed to the larger π-conjugated rigid structure and effective electron transition dipole moment in the former[18,19].

To verify the nuclear staining ability of TPI in cells, the fluorescence "turn-on" effects of TPI and DAPI were studied, as shown in Fig. 3. With increased DNA concentration, the UV titration exhibited an obvious hypochromic phenomenon. This is in contrast with the fluorescence titration, which displayed a clear hyperchromic effect with a small red-shift. According to previous theoretical findings, both hypochromicity and hyperchromicity imply the existence of an intercalative binding mechanism between the TPI molecules and DNA base pairs[20,21]. Meanwhile, both hypochromic and hyperchromic effects also occurred for the DAPI molecules in its UV absorption and fluorescence spectra, respectively. Notably, when the DNA concentration reached saturation ([DNA]:[TPI]>120:1), the

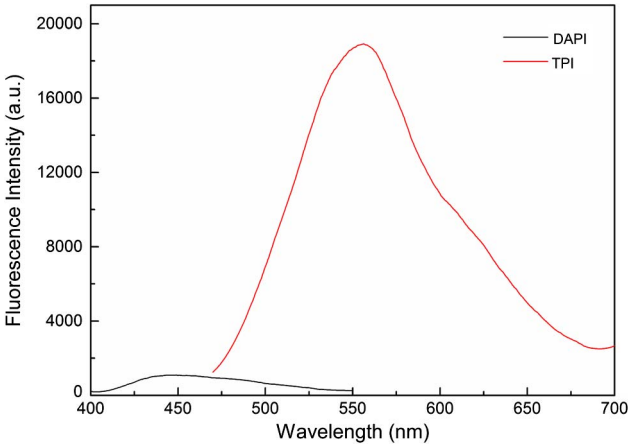

Fig. 2. Two-photon fluorescence spectra of TPI and DAPI in DMF, [TPI] = [DAPI] = 10^{-4} mol/L.

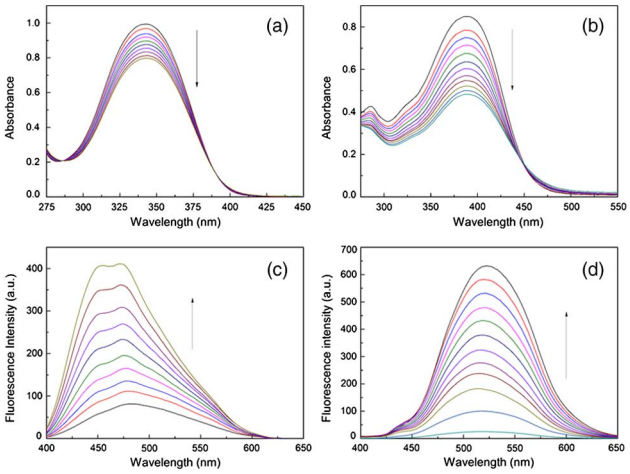

Fig. 3. (a) and (c) UV absorption and OPEF responses of DAPI and (b) and (d) TPI upon the titration of DNA in the Tris-HCl buffer solutions, [TPI] = [DAPI] = 10^{-5} mol/L, [DNA] = $0 - 1.3 \times 10^{-3}$ mol/L.

F of the TPI was enhanced by approximately 25-fold, which was five times higher than that of the DAPI. Simultaneously, a 15-fold enhancement of Φ was observed for the TPI before and after DNA titration in the buffer solutions. This fluorescence "turn-on" phenomenon can be attributed to the following factors. The water molecules inhibited the vibration of the TPI molecules and resulted in initial fluorescence quenching. However, the TPI molecules possessed good lipophilic properties because of the presence of terminal alcohol hydroxyl groups, along with their stable planar structure, and this prevented fluorescence quenching through intercalative binding among the basic groups[22]. Under these hydrophobic conditions, an increasingly larger number of TPI molecules were bound to the DNA basic groups, which led to the gradual enhancement of F.

The one- and two-photon fluorescence imaging results for TPI-stained 3T3 cells are shown in Fig. 4. Two colors (green and red) were used to represent the one-photon and two-photon fluorescence images, respectively, via built-in imaging software. The results showed that almost commensurable luminance intensities were emitted from both the OPEF and TPEF images, yielding an obvious yellow luminance in the merged images. However, the TPEF

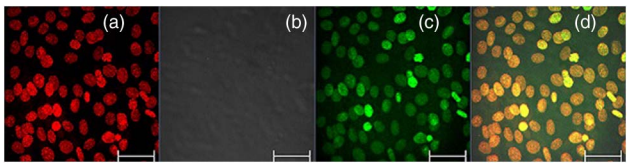

Fig. 4. One-photon and two-photon confocal fluorescence images of 3T3 cells stained with TPI (0.5 μmol/L) for 3 h. (a) TPEF bioimaging; (b) DIC picture; (c) OPEF bioimaging; (d) Merged bioimaging of a and c. The wavelength for two-photon and one-photon excitation was 800 and 405 nm, respectively. Scale bar was 50 μm.

imaging seemed to be clearer; this can be attributed to the superior signal-to-noise ratio and weaker background signal in the TPA process compared to the one-photon case.

In order to determine the nuclear localization ability of TPI in the 3T3 cells, a counterstain experiment was conducted using TPI co-stained with MTR. As shown in Fig. 5, the two fluorescent probes, TPI and MTR, displayed obvious selective labeling of nuclei and cytoplasms, respectively. The boundaries between the nuclei and cytoplasms were clearly visible as a result of the emission of green and red fluorescence from the two distinguishable intracellular positions. This result proved the following two points: firstly, the TPI probes could successfully penetrate the nuclei with excellent membrane permeability, exhibiting outstanding biocompatibility with the MTR in the complex intracellular environment; secondly, the TPI molecules could easily enter the nuclear pores, indicating that the molecular sizes were sufficiently small for binding with the DNA base pairs.

Photostability plays an extremely important role in the real-time monitoring of nuclei for two-photon bioimaging. Thus, the nuclear imaging of TPI- and DAPI-stained 3T3 cells from emission to extinction was conducted using a confocal scanning microscope. Images were taken at 30 s intervals, and the TPEF intensity values of the TPI and DAPI during successive laser irradiation were accurately recorded. As shown in Figs. 6–8, the TPI fluorescence duration from emission to extinction was approximately 1800 s, which was significantly longer than that of the DAPI (only ~900 s). The fluorescence attenuation amplitude (δ) within 300 s (T) was 8.5%. Compared with some of the latest reported probes, e.g., pyridine cation derivatives[15], T = 300 s, $\delta = 10\%$ and 20%; polypyridyl complexes[16], T = 300 s, $\delta = 38\%$; indole-based derivatives[22], T = 300 s, $\delta = 28\%$, it indicated that the TPI had better photostability. Furthermore, the TPEF intensity of the TPI was also higher at the same point in time, implying superior potential real-time observation resolution for nuclear bioimaging compared to the DAPI.

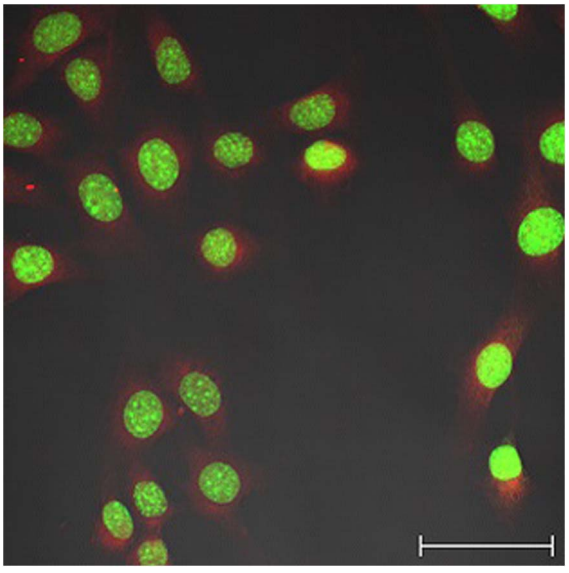

Fig. 5. Confocal fluorescence images of 3T3 cells co-stained with TPI (0.5 μmol/L) and MTR (0.5 μmol/L). For TPI, $\lambda_{ex} = 405$ nm, and $\lambda_{em} = 525 - 575$ nm. For MTR, $\lambda_{ex} = 575$ nm, and $\lambda_{em} = 585 - 660$ nm. Scale bar was 50 μm.

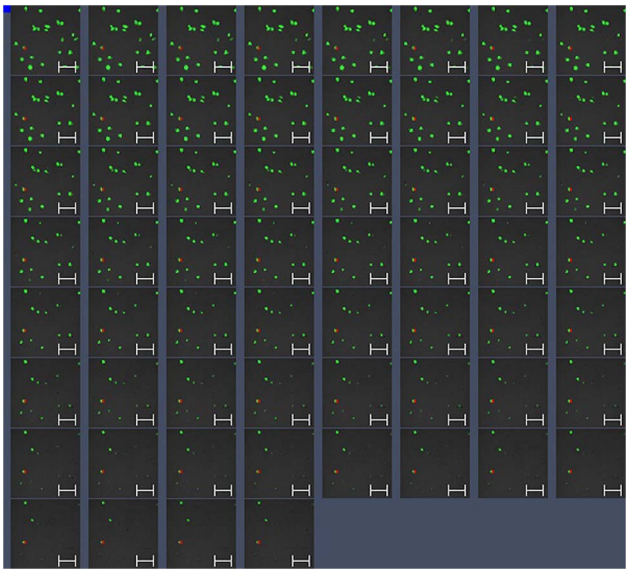

Fig. 6. Time-dependent confocal fluorescence bioimaging of 3T3 cells stained with TPI (0.5 μmol/L) for 15 min. The excitation wavelength was 800 nm. Scale bar was 50 μm.

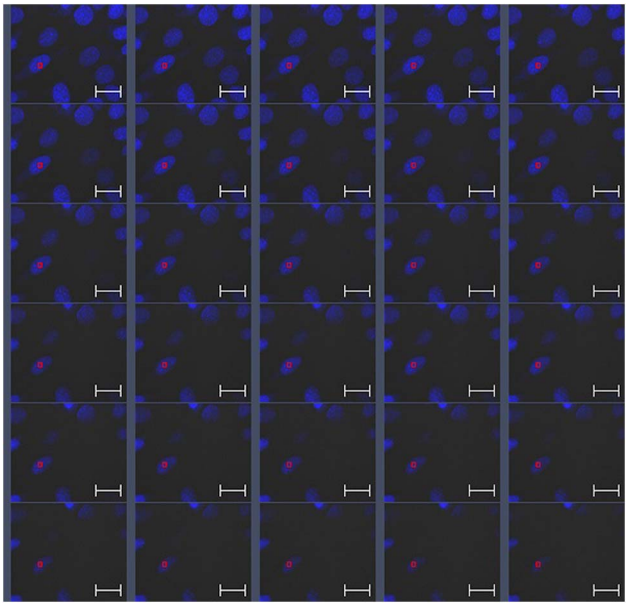

Fig. 7. Time-dependent confocal fluorescence bioimaging of 3T3 cells stained with DAPI (0.5 μmol/L) for 15 min. The excitation wavelength was 740 nm. Scale bar was 20 μm.

In conclusion, a novel dibenzothiophene-based TPEF probe is prepared and developed. Rigid conjugated-bridge dibenzothiophene is chosen as the central moiety, which is symmetrically connected to the functional pyridine

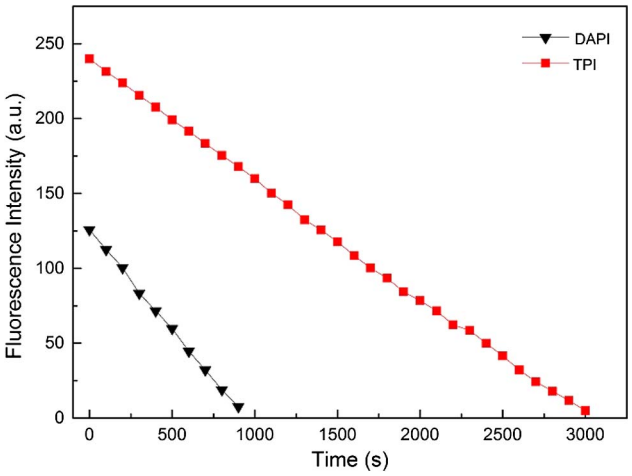

Fig. 8. Comparison of photostability of TPI and DAPI under successive irradiation.

groups. The 471 GM σ and 0.52 Φ suggest that this probe has promising applications in TPEF bioimaging. Further, the 25-fold enhancement of the fluorescence titration effect in buffer solutions indicates that the TPI has an obvious fluorescence "turn-on" effect. The TPEF bioimaging and counterstain experiment confirm the selective nuclear localization and two-photon imaging advantages of the developed probe. Finally, the 1800 s observation under successive femtosecond lasing indicates that the TPI has better photostability than that of DAPI. By virtue of its accurate nuclear staining level and stronger photostability, this novel dibenzothiophene-based fluorescent probe has potential application prospects in the field of two-photon fluorescence bioimaging.

This work was partially supported by the National Natural Science Foundation of China under Grant Nos. 61137002, 61178059, and 51172253.

References

1. Y. He, Z. Wang, Y. Wang, L. Wei, X. Li, J. Yang, G. Shi, and Y. Zhang, Chin. Opt. Lett. **13**, 111702 (2015).
2. J. J. Wang, Y. M. Sun, W. J. Zhang, Y. Liu, X. Q. Yu, and N. Zhao, Talanta. **129**, 241 (2014).
3. C. Q. Ye, B. Sun, X. M. Wang, J. W. Yang, P. Ding, S. J. Zhu, Q. G. He, Z. Q. Liang, and X. T. Tao, Dyes Pigm. **102**, 133 (2014).
4. K. D. Belfield, M. V. Bondar, C. O. Yanez, F. E. Hernandez, and O. V. Przhonska, J. Mater. Chem. **19**, 7498 (2009).
5. X. D. Zhang, H. X. Wang, H. Wang, Q. Zhang, J. F. Xie, Y. P. Tian, J. Wang, and Y. Xie, Adv. Mater. **26**, 4438 (2014).
6. Y. Ho, N. B. Au, K. Wong, C. Chan, W. Kwok, G. Law, K. Tang, W. Wong, C. Ma, and M. Lam, Chem. Commun. **50**, 4161 (2014).
7. F. Miao, G. F. Song, Y. M. Sun, Y. Liu, F. Q. Guo, W. J. Zhang, M. G. Tian, and X. Q. Yu, Biosens. Bioelectron. **50**, 42 (2013).
8. W. P. Ye, S. X. Wang, X. M. Meng, Y. Feng, H. T. Sheng, Z. L. Shao, M. Z. Zhu, and Q. X. Guo, Dyes Pigm. **101**, 30 (2014).
9. X. J. Feng, P. L. Wu, F. Bolze, H. Leung, K. F. Li, N. K. Mak, D. Kwong, J. Nicoud, K. Cheah, and M. S. Wong, Org. Lett. **12**, 2194 (2010).
10. J. Du, S. Deng, S. Hou, L. Qiao, J. Chen, Q. Huang, C. Fan, Y. Chen, and Y. Zhao, Chin. Opt. Lett. **12**, 041101 (2014).
11. E. Baggaley, M. R. Gill, N. H. Green, D. Turton, I. V. Sazanovich, S. W. Botchway, C. Smythe, J. W. Haycock, J. A. Weinstein, and J. A. Thomas, Angew. Chem. Int. Ed. **53**, 3367 (2014).
12. R. Wolleschensky, T. Feurer, R. Sauerbrey, and U. Simon, Appl. Phys. B **67**, 87 (1998).
13. Y. C. Zheng, M. L. Zheng, S. Chen, Z. S. Zhao, and X. M. Duan, J. Mater. Chem. B **2**, 2301 (2014).
14. Z. Q. Liu, D. X. Cao, Y. Chen, and Q. Fang, Dyes Pigm. **86**, 63 (2010).
15. F. Miao, W. J. Zhang, Y. Sun, R. Zhang, Y. Liu, F. Guo, G. Song, M. Tian, and X. Yu, Biosens. Bioelectron. **55**, 423 (2014).
16. W. Xu, J. Zuo, L. Wang, L. Ji, and H. Chao, Chem. Common. **50**, 2123 (2014).
17. G. Xu, D. Wei, J. Wang, B. Jiang, M. Wang, X. Xue, S. Zhou, B. Wu, and M. Jiang, Dyes. Pigm. **101**, 312 (2014).
18. T. H. Huang, X. C. Li, Y. H. Wang, Z. H. Kang, R. Lu, E. L. Miao, F. Wang, G. W. Wang, and H. Z. Zhang, Opt. Mater. **35**, 1373 (2013).
19. H. Y. Ahn, S. Yao, X. H. Wang, and K. D. Belfield, Appl. Mater. Interfaces. **4**, 2847 (2012).
20. X. M. Meng, W. P. Ye, S. X. Wang, Y. Feng, M. Chen, M. Z. Zhu, and Q. X. Guo, Sensor. Actuat. B-Chem. **201**, 520 (2014).
21. K. M. Zhang, W. Dou, P. X. Li, R. Chen, J. X. Ru, W. Liu, Y. M. Cui, C. Y. Chen, W. S. Liu, and D. C. Bai, Biosens. Bioelectron. **64**, 542 (2015).
22. Y. Liu, W. J. Zhang, Y. M. Sun, G. F. Song, F. Miao, F. Q. Guo, M. G. Tian, X. Q. Yu, and J. Z. Sun, Dyes Pigm. **103**, 191 (2014).